Analysis of a Compact Electrically Small Antenna with SRR for RFID Applications

Naveen Kumar Majji
Department of Electronics & Communication Engineering, KLEF, India | Department of Electronics & Communication Engineering, PSCMR College of Engineering and Technology, India
navvenkumarmajji@gmail.com

Venkata Narayana Madhavareddy
Department of Electronics & Communication Engineering, KLEF, India
mvn@kluniversity.in

Govardhani Immadi
Department of Electronics & Communication Engineering, KLEF, India
govardhanee_ec@kluniversity.in (corresponding author)

Navya Ambati
Department of Electronics & Communication Engineering, KLEF, India
ambatinavya88@gmail.com

Sree Madhuri Aovuthu
Department of Electronics & Communication Engineering, Rashtreeya Vidyalaya College of Engineering, India
asreemadhuri@gmail.com

Received: 19 September 2023 | Revised: 3 October 2023 | Accepted: 20 October 2023

Licensed under a CC-BY 4.0 license | Copyright (c) by the authors | *DOI: https://doi.org/10.48084/etasr.6418*

ABSTRACT

This paper contains the design and analysis of a compact, bidirectional Electrically Small Antenna (ESA) at 0.9 GHz for Radio Frequency Identification (RFID) and a global system for mobile communication applications. The proposed design consists of a microstrip patch antenna enclosed inside the split ring resonators, in which a split ring resonator was subtracted from the ground plane in order to obtain the results at lower frequencies by maintaining a compact size. This ESA was designed on FR4 substrate having a dimension of 30 mm × 30 mm × 1.6 mm. This antenna was created and simulated with the Ansys HFSS. The ESA was fabricated by chemical etching and it was measured with the MS2037C Anritsu Combinational Analyzer. The simulated results show that the ESA attains a bandwidth of 100 MHz (with S11 < -10 dB) at 0.9 GHz. The bidirectional radiation pattern in both H and E planes with a radiation efficiency of 80% at the resonant frequency was obtained. A close agreement of 90% between the simulated and the measured results was observed.

Keywords-electrically small antenna; microstrip patch; SRR; RFID applications

I. INTRODUCTION

Systems for Radio Frequency Identification (RFID) frequently employ microstrip antennas. Such systems have a wide range of practical uses in business, trade, transportation, biological research and clinical practice [1, 2]. An antenna and an RFIC are the only components of a passive tag. The devices that are designed by utilizing surface acoustic waves may be employed in wireless sensing applications (such as distance, temperature etc.) [3]. Most popularly available RFID tags for UHF and RF applications are designed with the help of electrically small antennas or standard half-wavelength planar dipole antennas [2, 4]. Implanted microwave technology is becoming more and more common for medical purposes [5, 6]. The electromagnetic signal degrades because of the medium around the implanted device has a high εr and a high δ. Due to the reduction of the dielectric medium properties effect, magnetic connection between the tag loop and the reader loop is preferred in this situation [6]. The loop dimensions employed inside biological media is often small, that is less than $\lambda/2$.

According to the third degree of the source's distance, the magnetic field dramatically decreases in the near-field zone [7]. To pick up a weakly backscattered response from the destination point, the microstrip antenna being used as a reader must provide a strong magnetic field. Typically, to do that, the microstrip patch dimensions must be increased. Building the patch as a periodically loaded line in order to realize an electrically small antenna is proposed in this paper. Between each leg of the loop, capacitors are routinely put as part of the line's architecture. The loop's electrical length is shortened as a result of the capacitive components' compensation for the phase incursion given by the inductive portions. The increased magnetic coupling is followed by a homogenous current distribution around the loop in this arrangement [8, 9]. To raise the tag read range while employing an ESA in the far-field area, the base station ESA should have superior radiation properties. ESAs are known to exhibit omnidirectional radiation in the loop plane. The reader antenna is intended to be built using an antenna module that combines a dipole with a non-interacting electrically small antenna. Additionally, this antenna's gain is twice as great as the gains of a single patch or single dipole antenna [9, 10]. The ESA is also small, which makes it useful for portable RFID scanners that communicate with conventional passive tags. In order to arbitrarily change the resonant frequency of a bowtie dipolar tag, the idea of integrating an inductive channel with a lumped external inductor was introduced in [25]. It was demonstrated that the inductive channel could readily control the currents flowing on the top-loading patch, and that channel width and an external lumped inductor could both be changed to efficiently alter the tag antenna's resonance frequency. The tag antenna, which has a two-layer construction and a high profile, cannot be read in all polarizations. A metal-mountable tag with many frequency tuning options has been created using two complementary C-shaped patches in [26]. The two patches are in close proximity in order to produce enough antenna reactance [27-28].

An ESA with a bidirectional radiation pattern for UHF RFID applications is proposed in this study. An SRR structure was utilized to minimize the size. The simulated results indicate that the electrically small antenna achieves bidirectional radiation pattern. There were no observable effects to the proposed antenna's resonance frequency, gain, and radiation pattern when they were stacked or tiled together.

II. ANTENNA DESIGN GEOMETRY

A. Methodology

The configuration and dimensions of the compact ESA are represented in Figure 1. It consists of a microstrip patch enclosed with SRRs in which a tile of microstrip transmission lines was subtracted from the microstrip patch. The microstrip ESA is engraved on FR4 material with 1.6 mm thickness and tanδ = 0.02. In addition to that, an SRR was subtracted from the ground plane with a dimension of 30 mm × 30 mm printed on the backside of the substrate. The complete geometry of the antenna is 30 mm × 30 mm × 1.6 mm and an impedance of 50 Ω is attached to the microstrip patch as excitation. The microstrip ESA with SRR was designed and simulated in Ansys HFSS and the properties of the material are represented in Table I. The dimensions utilized in designing the microstrip patch antenna are shown in Table II.

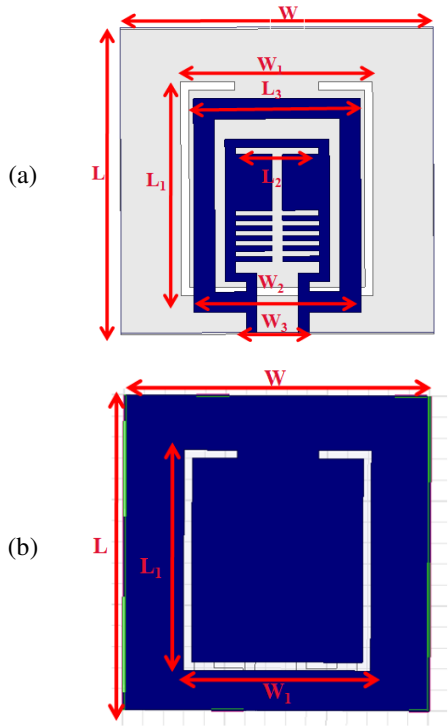

Fig. 1. Microstrip ESA with SRR: (a) Front view, (b) back view.

TABLE I. PROPERTIES OF MICROSTRIP ESA WITH SRR

Parameter	Value	Unit
Patch	Copper	-----
Thickness	1.6	mm
Density	8.96	gcm^{-3}
Electrical conductivity	58.7	siemens/m
Electrical resistivity	1.7	Ω.m
Thermal conductivity	386	W/m. K
Sheet resistance	0.5	mΩ/sq
Substrate	FR4 epoxy	-
Thickness	0.1	mm
Dielectric constant (ε_r)	4.4	-

TABLE II. DIMENSIONS OF THE PROPOSED MICROSTRIP ESA WITH SRR

Dimension	Value (mm)
Width of the ground plane (W)	30
Length of the ground plane (L)	30
Length of the microstrip Patch (L_1)	21
Width of the microstrip Patch(W_1)	16
Length of the microstrip Patch (L_2)	14
Width of the microstrip Patch (W_2)	12
Length of the microstrip Patch(L_3)	2
Width of the microstrip Patch (W_3)	1

B. Evolution Procedure

Figure 2 represents the evolutionary stages of the electrically small microstrip patch antenna with SRR structure. Antenna evolution process starts with the design of an ESA fed

by a 50 Ω microstrip transmission line (step 1). A rectangle of 16 mm width and 21 mm length was subtracted from the microstrip patch. Subsequently, a 14 mm × 2 mm rectangle was united to the patch antenna (the step 2). In step 4, the proposed antenna was designed with a full ground structure. In step 5, the microstrip antenna with the SRR structure in the ground plane is complete.

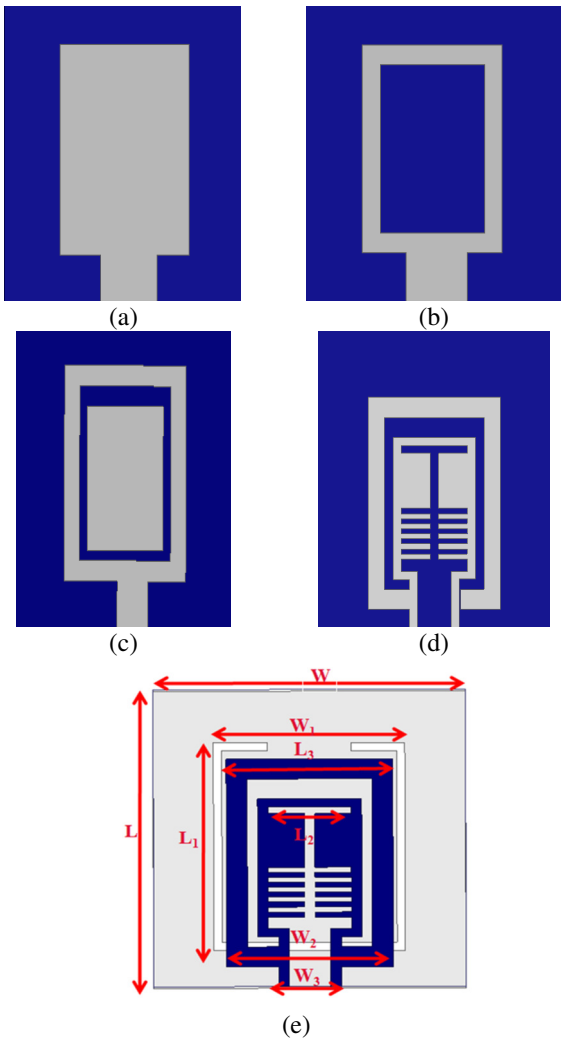

Fig. 2. Microstrip ESA with SRR. (a) Step 1, (b) step 2, (c) step 3, (d) step 4, (e) proposed design.

The dimensions of the microstrip patch antenna were calculated by utilizing the concept behind the theory of the transmission lines. The width of the patch can be calculated by:

$$W = \frac{V_o}{2F_r}\sqrt{\frac{2}{\varepsilon_r+1}} \quad (1)$$

The length of the patch can be calculated by (2), where ε_{reff} is the effective dielectric constant of the substrate:

$$L = \frac{c}{2F_r\sqrt{\varepsilon_{reff}}} - 2\Delta l \quad (2)$$

$$\Delta l = 0.412h\frac{(\varepsilon_{reff}+0.03)(w+0.26h)}{(\varepsilon_{reff}-0.258)(w+0.8h)}$$

The dielectric constant of the substrate is:

$$\varepsilon_{reff} = \frac{\varepsilon_r+1}{2} + \frac{\varepsilon_r-1}{2}\left[1+\left[\frac{12h}{w}\right]\right]^{-1/2} \quad (3)$$

where L and W are the length and width of the microstrip patch, h is the thickness of the FR4 substrate, v_0 is the velocity of light in free space and F_r is the resonant frequency of the antenna.

Figure 3 represents the simulated S11 of the microstrip ESA with SRR at different evolutionary stages. At the first step, the basic microstrip patch resonates at 0.8 GHz with a reflection co-efficient of -10 dB. At the second stage ESA resonates at 0.82 GHz with a S11 of -10 dB. In the third step antenna resonates at 0.85 GHz with a S11 of -16 dB and in addition to that antenna resonates at 2.3 GHz with a S11 of -11 dB. In step 4, the antenna without the SRR resonates at 0.87 GHz with a return loss of -20 dB and an additional band has been obtained at 2.3 GHz with a return loss of -12 dB. The final proposed antenna resonates at 900 MHz with a return loss of -22 dB, with an additional band obtained at 2.3 GHz having a return loss of -13 dB. As we have designed an electrically small antenna, we were not concentrated at 2.3 GHz and that is why we are discussing the resonant frequency of the antenna at 900 MHz by maintaining the lower size.

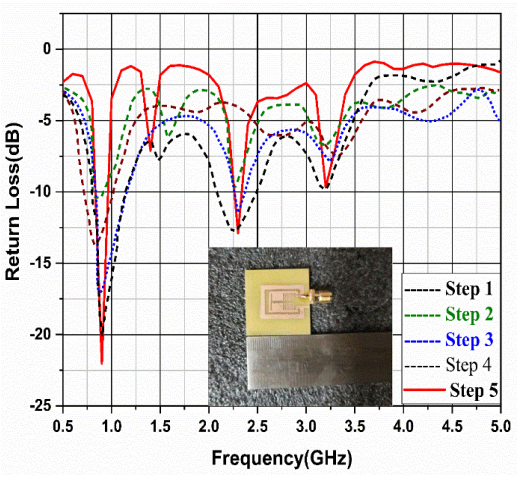

Fig. 3. Simulated return loss of the microstrip ESA with SRR at different evolutionary stages.

III. RESULTS AND DISCUSSION

Simulation of the proposed microstrip ESA with SRR was done by using Ansys HFSSv13 based on Finite Element Method (FEM) and Method of Moments (MOM). The microstrip ESA with SRR was excited by using a microstrip transmission line having a characteristic impedance of 50 Ω. To verify the simulated results were accurate, the proposed microstrip ESA was fabricated by using FR4 material as represented in Figure 4. The antenna fabrication was done by using chemical etching while parameters like reflection coefficient and VSWR of the antenna were measured with the MS2037C Anritsu Combinational analyzer. Radiation pattern

and gain of the antenna were measured with an Anechoic Chamber by utilizing antenna measurement equipment. Figure 5 shows the fabricated antenna measured with the combinational analyzer. Figure 6 shows the simulated and fabricated reflection coefficient of the microstrip ESA with split ring resonators.

(a) (b)

Fig. 4. Fabricated prototype of the Microstrip ESA with SRR.

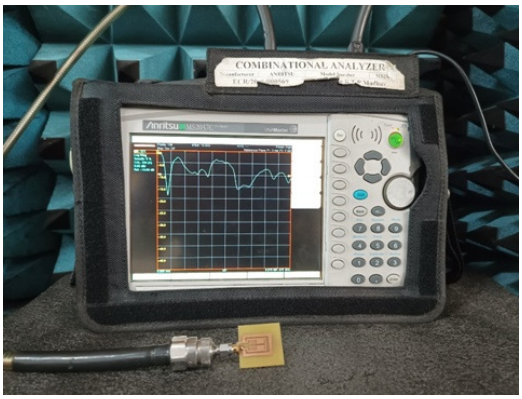

Fig. 5. Measurement of the Microstrip ESA with SRR.

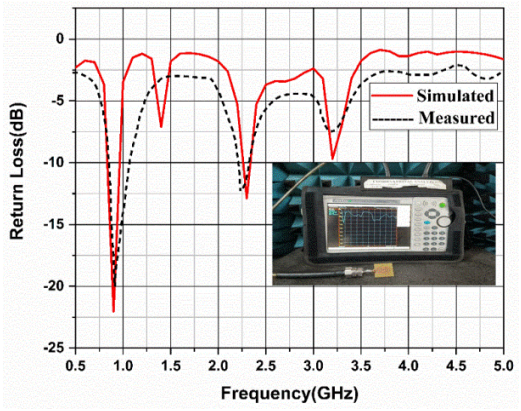

Fig. 6. Simulated and fabricated reflection coefficient of the Microstrip ESA with SRR.

From the return loss plot, it was observed that the simulated microstrip ESA with SRR resonates at 900 MHz with an S11 of -22 dB and the measured antenna resonates at 900 MHz with a reflection coefficient of -20 dB. Small deviation between the simulated and fabricated results due to connector and cable losses was detected.

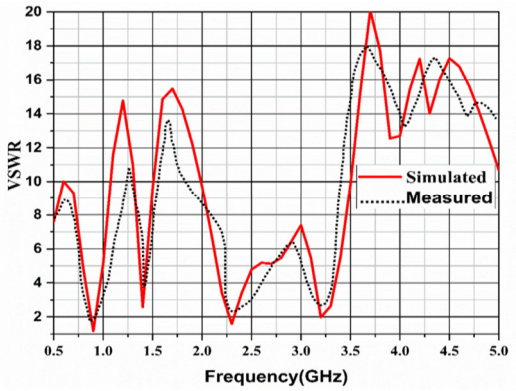

Fig. 7. Simulated and fabricated VSWR of the Microstrip ESA with SRR.

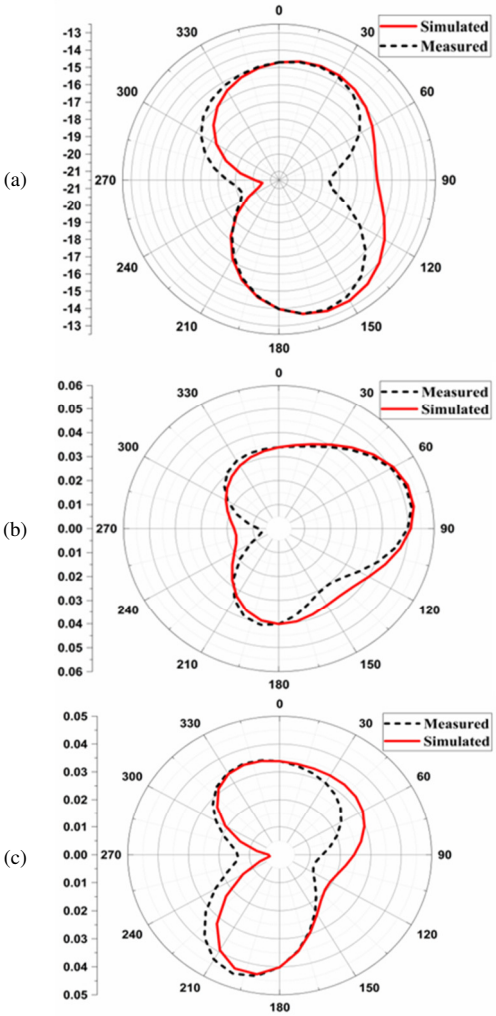

Fig. 8. Simulated and measured radiation pattern of the proposed ESA with SRR: (a) θ=0°, (b) θ=90°, (c) θ=180°.

Figure 7 shows the VSWR variation of the antenna with frequency. The proposed antenna resonates at 0.9 GHz. At the

resonant frequency, the simulated VSWR is 1.25 and the measured VSWR is 1.89. The radiation pattern was collected from an anechoic chamber employing antenna measurement equipment. A standard horn antenna is used as reference. Antenna efficiency of 80% is obtained by using the formula and selecting the values of incident and radiated power.

The radiation pattern is another significant antenna characteristic. Figures 8 and 9 demonstrate an antenna gain and the antenna radiation pattern. The minor variations between the fabricated and the simulated outcomes are caused by measurement and alignment issues.

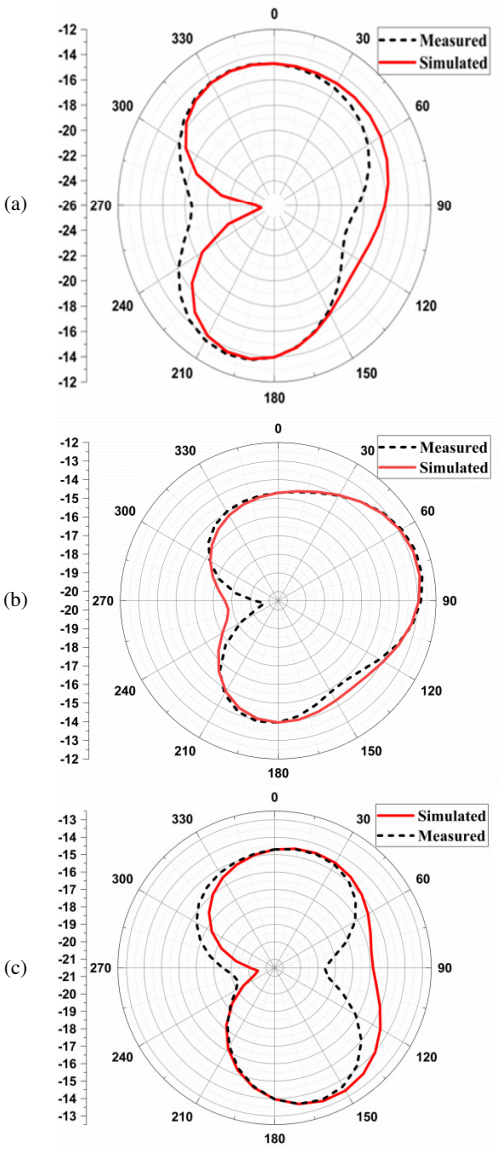

Fig. 9. Simulated and measured azimuthal radiation pattern of the proposed ESA with SRR: (a) ϕ=0°, (b) ϕ=90°, (c) ϕ=180°.

The E-field and current distribution of an electrically tiny circular ring antenna are shown in Figure 10. Maximum radiation is indicated by the red color, minimum radiation is indicated by the blue color, and the average distribution of surface currents is indicated by the green color. Figure 11 represents the measurement setup of the proposed antenna for measuring antenna parameters like gain and radiation pattern in an anechoic chamber. Figure 12 represents the 3D gain of the palanar microstrip ESA with SRR.

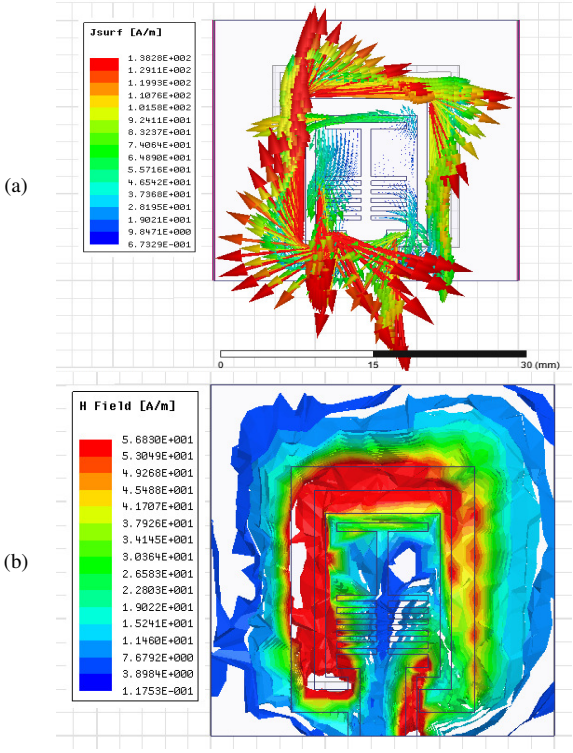

Fig. 10. Vector current and H-field distribution of the proposed microstrip ESA with SRR.

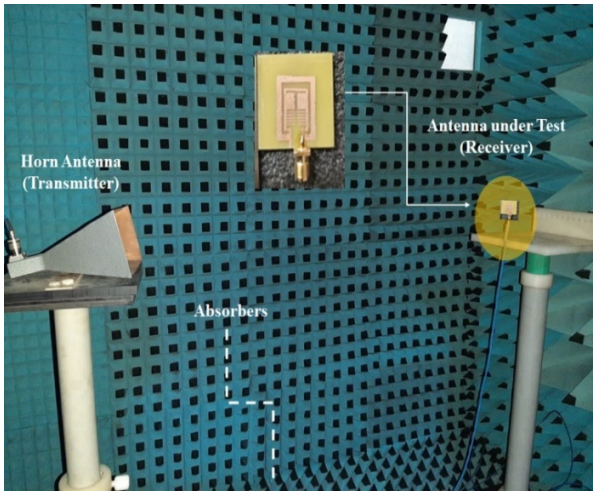

Fig. 11. Measurement setup of gain and radiation pattern.

Table III compares several previously published in literature antennas to the proposed broadband antenna for RFID applications. When compared to the proposed antenna, the

antenna suggested in [4] offered modest return loss. The antenna in [6] is huge in size and has a constrained impedance bandwidth. The antenna in [8] has a straightforward design and it offers less return loss and VSWR. According to [13], the antenna occupies more size and featured a complicated construction printed in Taconic RF-35. The comparison displays that the proposed broadband antenna has a number of benefits over earlier reported antennas [4–13] in terms of size, impedance bandwidth, and gain.

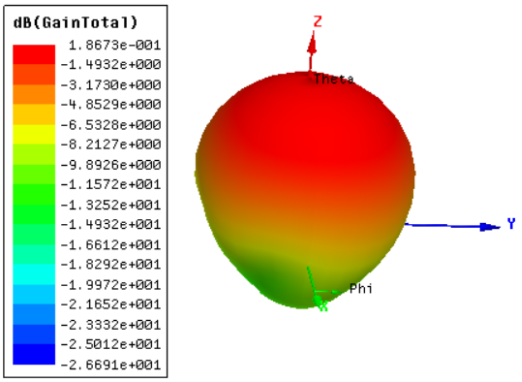

Fig. 12. 3D gain of the proposed microstrip ESA with SRR.

TABLE III. COMPARISON OF THE PROPOSED ANTENNA WITH OTHER KNOWN ANTENNAS

Ref.	Size (mm^3)	Material used	Resonant frequency	Return loss	VSWR
[24]	40×40×1.6	FR4	870 MHz	-10.1 dB	1.8
[25]	60×70×0.5	Rogers/RT Duroid 5880	890 MHz	-14 dB	1.89
[26]	50×50×0.8	FR4	900 MHz	-18 dB	1.78
[27]	40×40×1.5	Rogers/RT Duroid 5880	870 MHz	-12 dB	1.85
[28]	80×20×0.5	Taconic RF-35	1.7 GHz	-15 dB	1.55
Proposed	30×30×1.6	FR4	900 MHz	-22 dB	1.25

IV. CONCLUSION

A compact, bidirectional Electrically Small Antenna (ESA) resonating at 900 MHz was designed, simulated, and measured with the MS2037C Anritsu Combinational Analyzer and its simulated S11 is -22 dB at 900 MHz. The measured bandwidth S11 < -10 dB is 100 MHz. There is a good match between the simulated and the measured results in terms of VSWR and S11. Radiation pattern is bidirectional in both the azimuthal and elevation angles, thus, the proposed antenna is suitable for RFID applications and for mobile communication applications.

REFERENCES

[1] K. Finkenzeller, *RFID Handbook: Fundamentals and Applications in Contactless Smart Cards, Radio Frequency Identification and Near-Field Communication*, 3rd Edition. New York, NY, USA: John Wiley & Sons, 2010.

[2] K. V. S. Rao, P. V. Nikitin, and S. F. Lam, "Antenna design for UHF RFID tags: a review and a practical application," *IEEE Transactions on Antennas and Propagation*, vol. 53, no. 12, pp. 3870–3876, Sep. 2005, https://doi.org/10.1109/TAP.2005.859919.

[3] V. P. Plessky and L. M. Reindl, "Review on SAW RFID tags," *IEEE Transactions on Ultrasonics, Ferroelectrics, and Frequency Control*, vol. 57, no. 3, pp. 654–668, Mar. 2010, https://doi.org/10.1109/TUFFC.2010.1462.

[4] D. V. Kholodnyak, P. A. Turalchuk, A. B. Mikhailov, S. Yu. Dudnikov, and I. B. Vendik, "3D Antenna for UHF RFID Tags with Eliminated Read-Orientation Sensitivity," in *European Microwave Conference*, Manchester, UK, Sep. 2006, pp. 583–586, https://doi.org/10.1109/EUMC.2006.281459.

[5] J. C. Lin, *Electromagnetic Fields in Biological Systems*. Boca Raton, FL, USA: CRC Press, 2011.

[6] S. Rao *et al.*, "Miniature implantable and wearable on-body antennas: towards the new era of wireless body-centric systems," *IEEE Antennas and Propagation Magazine*, vol. 56, no. 1, pp. 271–291, Oct. 2014, https://doi.org/10.1109/MAP.2014.6821799.

[7] C. A. Balanis, *Antenna Theory: Analysis and Design*, 3rd Edition. Hoboken, NJ, USA: Wiley, 2005.

[8] D. Dobkin, S. M. Weigand, and N. Iyer, "Segmented magnetic antennas for near-field UHF RFID," *Microwave Journal*, vol. 50, no. 6, pp. 96–102, Jun. 2007.

[9] A. L. Popov, O. G. Vendik, and N. A. Zubova, "Magnetic field intensity in near field zone of loop antenna for RFID systems," *Technical Physics Letters*, vol. 36, no. 10, pp. 882–884, Oct. 2010, https://doi.org/10.1134/S1063785010100032.

[10] O. G. Vendik and I. A. Pakhomov, "Electric-and magnetic-field strengths in the Fresnel zone of a microradiator formed by an electric and a magnetic dipole," *Technical Physics*, vol. 50, no. 11, pp. 1479–1484, Nov. 2005, https://doi.org/10.1134/1.2131958.

[11] A. Shvetsov *et al.*, "Choice of quartz cut for sensitive wireless SAW temperature sensor," in *IEEE International Ultrasonics Symposium*, Chicago, IL, USA, Sep. 2014, pp. 1505–1508, https://doi.org/10.1109/ULTSYM.2014.0372.

[12] L. J. Chu, "Physical Limitations of Omni-Directional Antennas," *Journal of Applied Physics*, vol. 19, no. 12, pp. 1163–1175, Apr. 2004, https://doi.org/10.1063/1.1715038.

[13] P. A. Turalchuk, D. V. Kholodnyak, and O. G. Vendik, "A novel low-profile antenna with hemispherical coverage suitable for wireless and mobile communications applications," in *Loughborough Antennas and Propagation Conference*, Loughborough, UK, Mar. 2008, pp. 337–340, https://doi.org/10.1109/LAPC.2008.4516935.

[14] I. Govardhani *et al.*, "Design of high directional crossed dipole antenna with metallic sheets for UHF and VHF applications," *International Journal of Engineering & Technology*, vol. 7, no. 1.5, Dec. 2017, Art. no. 42, https://doi.org/10.14419/ijet.v7i1.5.9120.

[15] G. Imamdi, M. Narayan, A. Navya, and A. Roja, "Reflector array antenna design at millimetric (mm) band for on the move applications," *ARPN Journal of Engineering and Applied Sciences*, vol. 13, no. 1, pp. 352–359, Jan. 2018.

[16] G. Immadi *et al.*, "Analysis of substrateintegrated frequency selective surface antenna for IoT applications," *Indonesian Journal of Electrical Engineering and Computer Science*, vol. 18, no. 2, May 2020, Art. no. 875, https://doi.org/10.11591/ijeecs.v18.i2.pp875-881.

[17] M. Naveen Kumar, M. Venkata Narayana, G. Immadi, P. Satyanarayana, and A. Navya, "Analysis of a low-profile, dual band patch antenna for wireless applications," *AIMS Electronics and Electrical Engineering*, vol. 7, no. 2, pp. 171–186, 2023, https://doi.org/10.3934/electreng.2023010.

[18] K. H. Reddy, M. V. Narayana, G. Immadi, P. Satyanarayana, K. Rajkamal, and A. Navya, "A Low-profile Electrically Small Antenna with a Circular Slot for Global Positioning System Applications," *Progress In Electromagnetics Research C*, vol. 133, pp. 27–38, 2023, https://doi.org/10.2528/PIERC23021601.

[19] H. R. Katireddy, M. V. Narayana, and G. Immadi, "Innovative Design and Analysis of an Electrically Small Reconfigurable Antenna for GPS and Blue Tooth Applications," *Engineering, Technology & Applied Science Research*, vol. 11, no. 5, pp. 7684–7688, Oct. 2021, https://doi.org/10.48084/etasr.4465.

[20] M. O. Dwairi, "Increasing Gain Evaluation of 2×1 and 2×2 MIMO Microstrip Antennas," *Engineering, Technology & Applied Science*

Research, vol. 11, no. 5, pp. 7531–7535, Oct. 2021, https://doi.org/10.48084/etasr.4305.

[21] S. Sarade and S. D. Ruikar, "Development of a Wide Bandwidth Massive Eight Dissimilar Radiating Element Multiband MIMO Antenna for mm-Wave Application," *Engineering, Technology & Applied Science Research*, vol. 12, no. 5, pp. 9166–9171, Oct. 2022, https://doi.org/10.48084/etasr.5133.

[22] M. Venkateswara Rao, B. T. P. Madhav, J. Krishna, Y. Usha Devi, T. Anilkumar, and B. Prudhvi Nadh, "CSRR-loaded T-shaped MIMO antenna for 5G cellular networks and vehicular communications," *International Journal of RF and Microwave Computer-Aided Engineering*, vol. 29, no. 8, 2019, Art. no. e21799, https://doi.org/10.1002/mmce.21799.

[23] K. V. Vineetha, P. R. Kumar, A. N. Babu, J. B. Naik, B. T. P. Madhav, and S. Das, "Investigations on Complementary Split Ring Resonator (CSRR) array integrated printed conformal band pass filters for modern wireless communication applications," *Journal of Instrumentation*, vol. 17, no. 10, Jul. 2022, Art. no. P10043, https://doi.org/10.1088/1748-0221/17/10/P10043.

[24] M. Najumunnisa *et al.*, "A Metamaterial Inspired AMC Backed Dual Band Antenna for ISM and RFID Applications," *Sensors*, vol. 22, no. 20, Jan. 2022, Art. no. 8065, https://doi.org/10.3390/s22208065.

[25] S.-M. Chiang, E.-H. Lim, P.-S. Chee, Y.-H. Lee, and F.-L. Bong, "Dipolar Tag Antenna With a Top-Loading Inductive Channel With Broad Range Frequency Tuning Capability," *IEEE Transactions on Antennas and Propagation*, vol. 70, no. 3, pp. 1653–1662, Mar. 2022, https://doi.org/10.1109/TAP.2021.3111093.

[26] M. Murugesh, E.-H. Lim, P.-S. Chee, and F.-L. Bong, "Complementarily Coupled C-Shaped Microstrip Patches With Wide-Range Frequency Tuning Capability for Metal-Applicable UHF RFID Tag Design," *IEEE Transactions on Antennas and Propagation*, vol. 70, no. 12, pp. 11548–11558, Sep. 2022, https://doi.org/10.1109/TAP.2022.3209733.

[27] T. Althobaiti, A. Sharif, J. Ouyang, N. Ramzan, and Q. H. Abbasi, "Planar Pyramid Shaped UHF RFID Tag Antenna With Polarisation Diversity for IoT Applications Using Characteristics Mode Analysis," *IEEE Access*, vol. 8, pp. 103684–103696, 2020, https://doi.org/10.1109/ACCESS.2020.2999256.

[28] W.-H. Ng, E.-H. Lim, F.-L. Bong, and B.-K. Chung, "Compact Folded Crossed-Dipole for On-Metal Polarization Diversity UHF Tag," *IEEE Journal of Radio Frequency Identification*, vol. 4, no. 2, pp. 115–123, Jun. 2020, https://doi.org/10.1109/JRFID.2020.2965282.